Research in Astronomy and Astrophysics, 25:025017 (9pp), 2025 February

https://doi.org/10.1088/1674-4527/ad942a
CSTR: 32081.14.RAA.ad942a

Research on Adjustable Cold View Field Diaphragm in Optical System with Linear Array Detector in AIMS

Lianwei Zhao, Meng Mou, Zhanhu Wang, Qing Fan, Chenjun Zhang, Jianwen Hua, and Lei Ding
Shanghai Institute of Technical Physics, Chinese Academy of Sciences, Shanghai 200080, China; lwzhao@mail.sitp.ac.cn
Received 2024 October 25; accepted 2024 November 11; published 2025 February 12

Abstract

The infrared Fourier transform spectrometer needs a cold view field diaphragm to reduce stray radiation. For an infrared spectrometer with linear array detectors, the part of the view field diaphragm where the light passes can be regarded as a slit. If the infrared detectors are small in size, the width of the slit is also small, which will cause serious diffraction phenomena. If the widths of the view field diaphragm and the optical system are designed by geometric optics theory, the diffraction light cannot be fully received by the detectors, which will cause energy loss. Expanding the width of the view field diaphragm will introduce stray radiation. Meanwhile, spectrometer follow-up optics should be set in cold environments to reduce the infrared background of the instrument. Optical materials have different thermal characteristics, the optical and mechanical structures will deform at low-temperature, and the cold view field diaphragm is installed at room temperature, so it is impossible to guarantee that the cold view field diaphragm remains in its design position when working at low-temperature. This paper solves the above problems by designing an adjustable cold view field diaphragm installed in its cryogenic vacuum chamber. The width and position of the view field diaphragm can be adjusted when working in cold temperatures, without opening the cryogenic vacuum chamber. Contrasting the interference signal obtained by the detectors in the adjustment process, the system can get the most suitable width and position of the cold view field diaphragm. The above works are based on the spectrometer used in the study named Accurate Infrared Magnetic Field Measurements of the Sun.

Key words: instrumentation: interferometers – instrumentation: detectors – Sun: infrared – Sun: magnetic fields

1. Introduction

Infrared optical instruments often use cold optical technology to reduce thermal infrared background noise while detecting fine spectra of targets (Ma et al. 2017). Cold light shields, light-blocking rings, and eliminating stray light diaphragms are often installed in infrared optical systems to suppress the influence of stray light and improve the system's signal-to-noise ratio (Wang et al. 2015). Because of the different thermal performance of optical and mechanical structures between room temperature and low-temperature, it is difficult to guarantee the low-temperature optical performance of the system directly by precise design, error analysis, or material analysis (Wang et al. 2022). Processing and assembly errors can also affect the optical and mechanical structures' low-temperature dimensional and positional accuracy. For view field diaphragms with high positioning accuracy requirements and small size, the low-temperature size and position have a more significant impact on signals.

OKSI Corporation in the United States achieved the real-time adjustment of a cold diaphragm by setting an external variable diaphragm. The diaphragm is driven by a worm gear and a motor. This method required special large cooling capacity refrigeration machines to cool the adjustable diaphragm (Nahumn et al. 2007; Sun et al. 2024). In 2014, the Changchun Institute of Optics, Fine Mechanics, and Physics invented an infrared variable diaphragm mechanism, in which the detectors, an aperture disk, and a filter disk were integrated into a dewar vessel. Different sizes of diaphragms were installed on the diaphragm disk, and different frequency band filters were installed on the filter disk. Switching the diaphragm disk and the filter disk in the mechanism could achieve the adjustment. However, in this method, the diaphragm size could not be continuously adjusted. For the view field diaphragm at the micrometer level, the diffraction effects would seriously impact image quality. In Wei et al. (2020), a mechanism was designed to compensate for the adverse impact of view field diaphragm diffraction. This method is suitable for room temperature applications.

This paper explores the method and device for both width and position continuous adjustment of a cold view field diaphragm, and the process is real-time. The width and position of the view field diaphragm are determined based on the signal strength and instrument performance of the spectrometer. In this method, the instrument performance could be optimized.

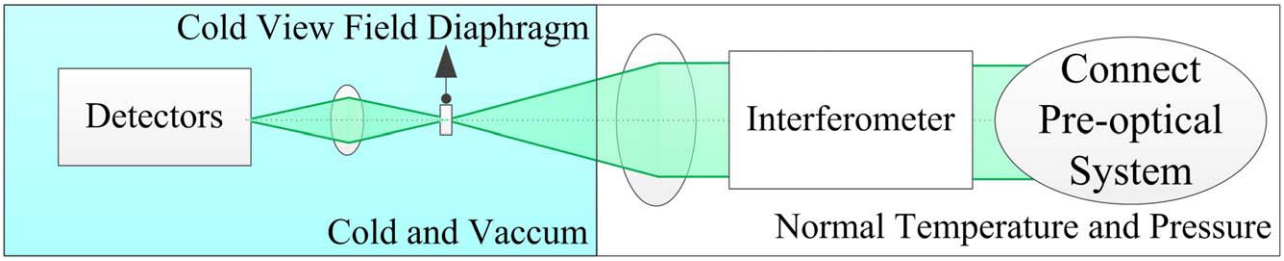

Figure 1. Schematic of instrument optics principle.

2. Research on the Application of View Field Diaphragm

2.1. The Necessity of Adjustable Width in the View Field Diaphragm

For linear array detectors, if the view field diaphragm is designed by theory calculation, the diffraction phenomenon of the beam is more obvious at the optical image plane, and especially for small-size detectors, the longer the wavelength is, the stronger the diffraction effect will be. In ideal applications, all diffraction beams can be fully received by the detectors without any energy loss if the spectrometer follow-up optics system is large enough. In practical applications, the optimal component size in the optical system is often designed based on geometric optics. So, it is difficult for spectrometer follow-up optics to collect all diffraction beams onto the detectors, and this will cause energy loss. Meanwhile, the diffraction beams from nearby view fields will shine onto the detector, which will introduce stray light. Increasing the width of the view field diaphragm to reduce the diffraction effect of the beam would bring in the light outside the view field, and that light will become the stray light after multiple scatterings. The stray light incident onto the detectors will increase noise and decrease the system's signal-to-noise ratio. Therefore, for linear array imaging systems, if the detector pixel is small and the detection wavelength is long, the width of the view field diaphragm will significantly impact system performance. As the introduction states, the optimal width of the view field diaphragm cannot be obtained through design. Thus, the width of the cold view field diaphragm must be adjustable.

2.2. The Necessity of Position Adjustment in Cold View Field Diaphragm

Using low-temperature optical technology to reduce the temperature of the optical system can effectively reduce background noise, and improve signal-to-noise ratio and sensitivity. Usually, the optical system has installation errors, accurate data on the deep low-temperature thermal expansion coefficient of materials are absent, and the user is unable to accurately calculate the deformation of the optical structure at low-temperature. So, the position of the view field diaphragm installed at room temperature is often no longer in the design position when the view field diaphragm is set in a low-temperature environment. Therefore, to obtain the optimal position of the cold view field diaphragm, it is ideal to design the diaphragm that is adjustable during low-temperature operation.

2.3. Application Examples of Cold View Field Diaphragm

For the study named Accurate Infrared Magnetic Field Measurements of the Sun (AIMS) (supported by the National Natural Science Foundation of China (NSFC, Grant No. 11427901)), the fore-optical system is a solar telescope that introduces sunlight into the "Fourier Transform Infrared Spectrometer" (FTIR). After passing through the interferometer, the sunlight is incident on the detectors in FTIR. FTIR can convert the sunlight signals into electrical signals, and then AIMS can obtain the spectral signal through Fourier inversion of interference signals. In the FTIR, each detector element corresponds to a front view field of $1\farcs5$, the arrangement array of detectors is 64 rows $\times$ 2 columns, each detector chip size is 50×50 μm, and there is a distance of 50 μm between the two columns of detector chips. The detection spectrum is the Sun spectrum near 12.32 μm.

In FTIR, the view field is small, the detector pixel resolution is high, and the detection spectral bandwidth is narrow, so the signal obtained by one detector chip is very small. To improve the signal-to-noise ratio of the instrument, the optical structures such as the view field diaphragm and filter wheel should be working in an 80 K environment, meanwhile, the effects of energy loss and infrared stray light should be considered too. The detector chip has a small size, so the view field diaphragm at the conjugate of the optical image plane of the detector chip can be regarded as a narrow single slit, and the optical positioning accuracy at low-temperature is high. The optical principle of this instrument is illustrated in Figure 1. Based on the above analysis, the cold view field diaphragm in FTIR should be adjustable, and contrasting the interference signal obtained by the detectors in the adjustment process, AMIS can get the most suitable width and position of the cold view field diaphragm.

3. Adjustment Method of Cold View Field Diaphragm

3.1. Research on the Adjustment Method of Cold View Field Diaphragm

The above analysis points out the necessity of using a cold adjustable slit diaphragm in a high spectral resolution infrared spectrometer while detecting the thermal infrared band, especially for spectrometers with linear array detector chips. There are many methods to adjust the view field diaphragm at room temperature, but these methods cannot be directly used for low-temperature situations. There are few methods for adjusting a low-temperature slit diaphragm, and this paper aims to explore a technique for adjusting a low-temperature slit diaphragm.

Considering the view field diaphragm is placed in a low-temperature environment, a vacuum environment is essential. The entire adjustment mechanism must be placed in a closed cryogenic vacuum chamber, and manual adjustment slits sold on the market are not suitable. If a motor-driven device is used to adjust the low-temperature diaphragm, there are the following unfavorable factors:

1. The adjustable device needs to be equipped with a low-temperature vacuum motor and vacuum connectors, and also a motor controller that operates at room temperature is required. This device has both mechanical and electrical components, parts of the device are inside the cryogenic vacuum chamber and parts are outside the cryogenic vacuum chamber, the structure is distributed, and the volume is large, however, the cost is not low.
2. Generally, small vacuum motors have very low torque. It is necessary to add vacuum grease to the transmission device to overcome the resistance torque. After long-term operation, the vacuum grease will pollute the optical components when slowly evaporating.
3. A low-temperature vacuum displacement measurement device needs to be installed to determine the amount of adjustment for the view field diaphragm. Common sensors and electronic devices cannot work at low-temperature (such as 80 K).

Also, replacing the view field diaphragm with a series of different sized slits can accomplish the adjustment, and we select the slit with the best effect after a series of experimental test results. However, this method is cumbersome and time-consuming to operate: the process of replacing the slit requires opening the cryogenic vacuum chamber repeatedly, and before opening the cryogenic vacuum chamber, first, it is necessary to perform reheating and vacuum re-pressing operations on the cryogenic vacuum chamber, then open the cryogenic vacuum chamber to replace the slit, after that, heating and cleaning the inside of the cryogenic vacuum chamber, at last evacuating the cryogenic vacuum chamber and gradually cooling it down. The cryogenic vacuum chamber has insulation structures such as a cold screen and a multi-layer insulation structure. When replacing the narrow slit, the insulation structure needs to be reinstalled. The process of replacing the narrow slit is very long and involves many steps, and the optimal effect cannot be achieved due to the discontinuous size of the replacement slit.

After studying this problem, using a pure mechanical adjustable cold view field diaphragm can avoid the aforementioned adverse factors and obtain the optimal diaphragm position and slit width. The method is as follows: using a micrometer head as the adjustment and displacement measurement component, using bellows as the sealing component, using two movable blades to form a slit, using screws to pre-adjust the initial position, and using flexible cold chains to cool the blades. Below are the specific implementation mechanisms and adjustment methods.

3.2. Implementation Mechanism for Adjustable Cold View Field Diaphragm

3.2.1. Overall Mechanism for Adjustable Cold View Field Diaphragm

The view field diaphragm adjustment mechanism is illustrated in Figure 2, including bellows, diaphragm linkages, adiabatic tubes, micrometer heads, etc. The diaphragm linkage and adiabatic tube are made of titanium alloy material, and the radial thickness of the adiabatic tube is 0.2 mm to reduce heat loss. One end of the adiabatic tube is connected to the bellows through threads, and the other is connected to the diaphragm linkage through threads. The relative position between the adiabatic tube and the diaphragm linkage is fixed using a locking nut. The bellows are fixed on the cryogenic vacuum chamber through a flange, and the connection is sealed with silver wire. Blades with sharp edges are designed on diaphragm linkage 1 and diaphragm linkage 2, the blades composing the two sides of the view field diaphragm. Blade 1 and blade 2 form a narrow diaphragm, with the middle gap being the transparent part. The micrometer head applies force to the rod core, compresses the bellows, and drives the diaphragm linkages to move left and right. In this way, the positions of blade 1 and blade 2 can be adjusted, and the optimal width and position of the view field diaphragm are determined by the signals obtained by the detector chips.

3.2.2. Characteristic Requirements and Structure of the Bellows

The bellows should have appropriate stiffness while adjusting the view field diaphragm. If the stiffness is too high, the micrometer head must apply excessive force and is prone to get stuck during adjustment. Conversely, the diaphragm link is easy to swing with the bellows if the stiffness is too small. The size of the bellows should be as small as possible to save space.

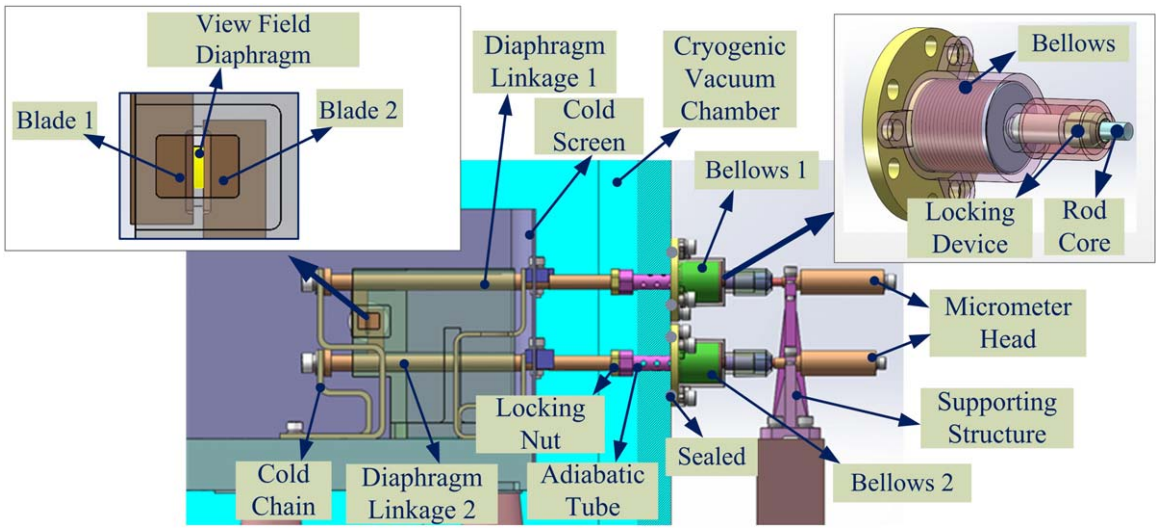

Figure 2. Diagram of the view field diaphragm adjustment mechanism.

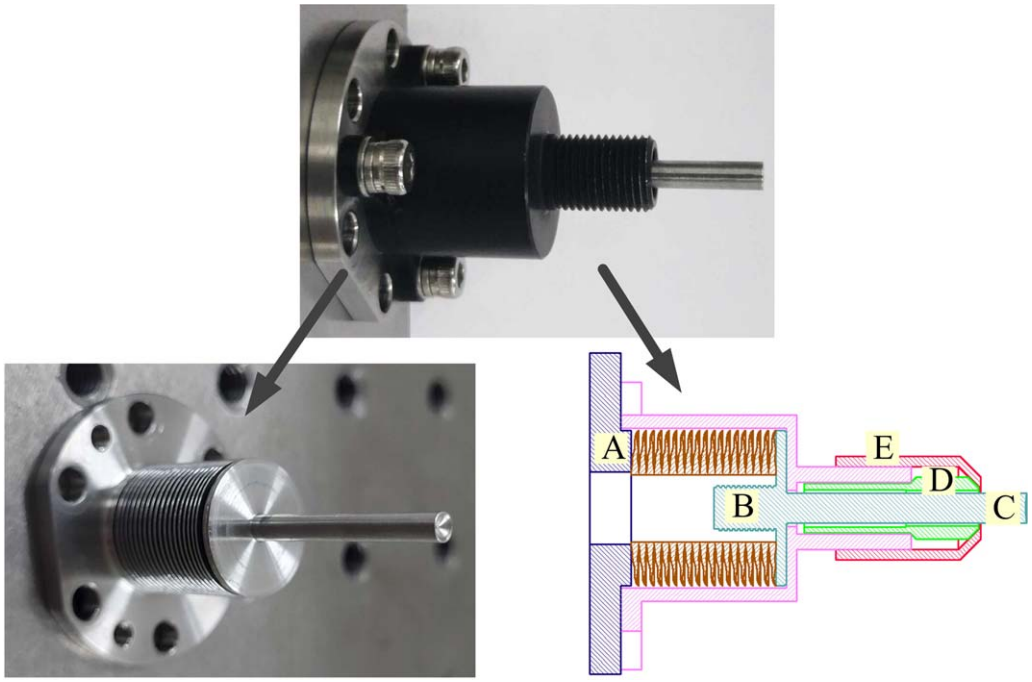

Figure 3. Structural diagram of the bellows.

The amount of compression should meet the adjustment requirement of the view field diaphragm slit.

The bellows adopt a stacked waveform to generate large displacements, and this shape can withstand large loads under external pressure. The bellows are designed with variables such as the thickness of the ripple, the number of ripples, and the ratio of outer diameter to inner diameter. The structure of the bellows is depicted in Figure 3, and the bellows are fixed on the wall of the cryogenic vacuum chamber through flange A. The B-end of the rod core has external threads to connect the adiabatic tube, and it can also adjust the relative position between the adiabatic tube and the bellows. The length of the B-end thread is greater than the

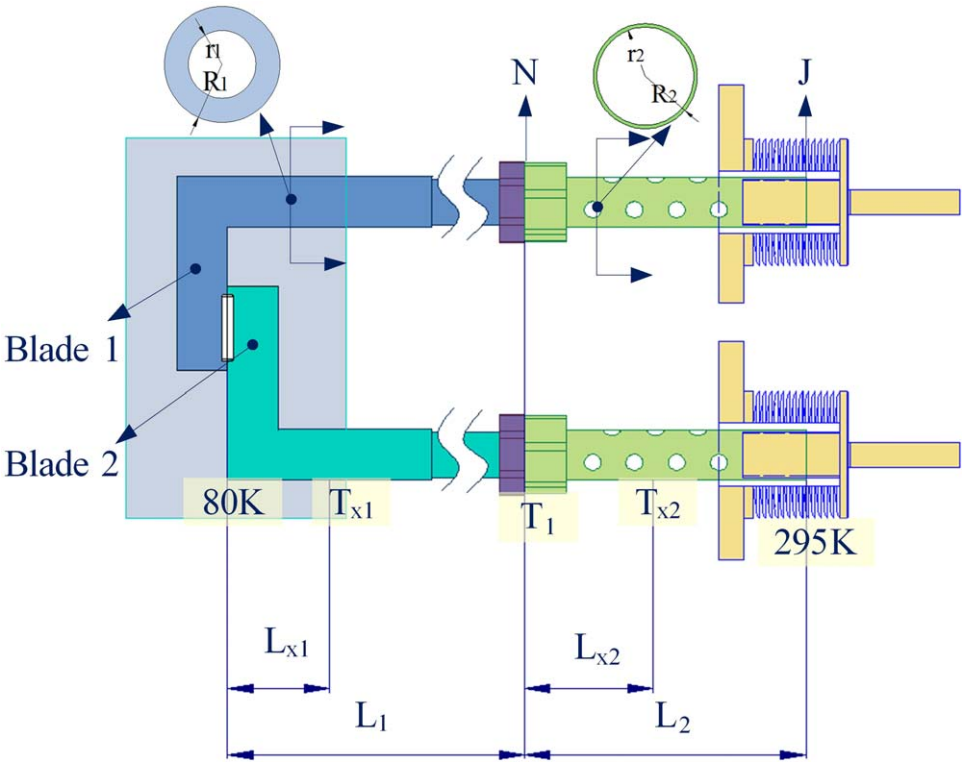

Figure 4. Schematic of temperature for each position of the view field diaphragm.

total adjustment amount of the view field diaphragm. The micrometer head is forced on the C-end of the rod core. D and E are a locking device that can fix the position of the rod core and maintain the compression of the bellows.

3.2.3. Cold Position Calculation of View Field Diaphragm Blade

The temperature in the cryogenic vacuum chamber will be cooled down from room temperature to low-temperature, and during this process, the diaphragm linkage and the adiabatic tube will be cooled down. Due to the cold shrinkage, the blades will be moved toward the bellows, and this process will change the initial position of the blades. This displacement amount needs to be compensated when designing the structure parameters. A cold screen is installed between the low-temperature optical system and the cryogenic vacuum chamber, and the cold screen is covered with a multi-layer insulation structure. So, the thermal radiation of the optical components inside the cryogenic vacuum chamber can be ignored, and only thermal conduction is considered. As illustrated in Figure 4, the side of the diaphragm linkage near the blade is connected to the cold chain. The temperature at blade 1 and blade 2 on the diaphragm linkages is 80 K, and the end of the adiabatic tube J is connected to the bellows at a temperature of 295 K. According to the heat conduction formula, the heat Q_N for the connection position N between the diaphragm linkage and the adiabatic tube can be expressed as

$$Q_N = KS_1\frac{T_1 - 80}{L_1} = KS_2\frac{295 - T_1}{L_2}. \quad (1)$$

In the formula, the thermal conductivity coefficient K is 7.2 W/(m·K), the distance L_1 from the blade to the end of the diaphragm linkage N is 109.75 mm, and the length of the adiabatic tube L_2 is 37 mm. The inner radius of the diaphragm linkage r_1 is 0.875 mm, the outer radius R_1 is 1.75 mm, and the heat transfer area S_1 can be expressed as $\pi(R_1^2 - r_1^2)$. The inner radius of the adiabatic tube r_2 is 0.875 mm, the outer radius R_2 is 1.475 mm, and the heat transfer area S_2 can be expressed as $\pi(R_2^2 - r_2^2)$. T_1 is the temperature at N, calculated by Equation (1): $T_1 = 210.592$ K, and the cooling loss generated by the adjustment mechanism is 0.062 W.

At low-temperature, the blade moves slightly to the right because of cold shrinkage of the diaphragm linkage and adiabatic tube. The amount of the movement is

$$\Delta L = \int_0^{L_1} \alpha(295 - T_{x1})dL_{x1} + \int_0^{L_2} \alpha(295 - T_{x2})dL_{x2}. \quad (2)$$

In the formula, the coefficient of thermal expansion of the material α is 8.8×10^{-6}/K, T_{x1} is the temperature at any

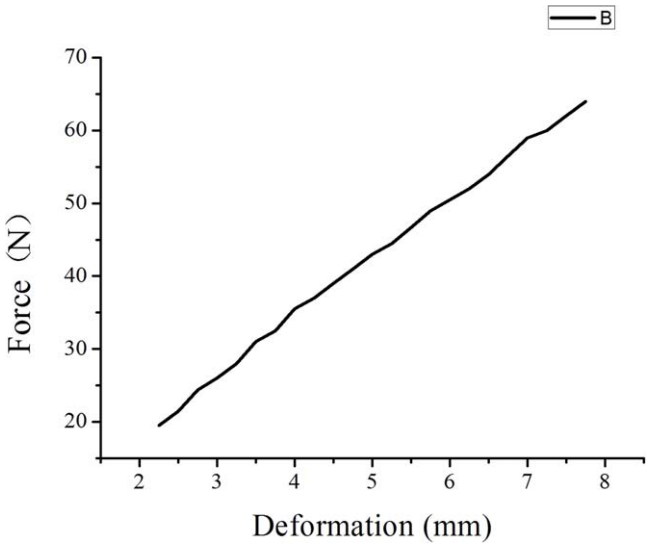

Figure 5. Characteristic Curve of Bellows.

position L_{x1} on the diaphragm linkage, and T_{x2} is the temperature at any position L_{x2} on the adiabatic tube. After calculation, in the cold state, both blade 1 and blade 2 move to the right along the initial design position by $\Delta L = 0.137$ mm due to cold shrinkage.

3.3. Cold View Field Diaphragm Adjustment

Analyze the thrust the bellows received under compression: the blade is mechanically positioned and fixed to the theoretical design position when installing the adjustment device. At room temperature, the bellows have an initial compression amount of X_0. At this time, blade 1 and blade 2 are tightly attached, and the view field diaphragm is in a closed state. Before adjustment, the displacement ΔL of the blades caused by the cold shrinkage of the diaphragm linkage and the adiabatic tube should be compensated. At this time, the compression amount of both bellows is $X_0+\Delta L$. When adjusting, twisting the micrometer head to push the rod core of the bellows to produce axial displacement, the blade can move from left to right. When the compression amount of the bellows increases, the blade moves left, and when the compression amount of the bellows decreases, the blade moves right. The blade's left and right adjustment amounts can be read from the micrometer head.

Denoting the maximum distance blade 1 can move to the left as X, where X is the position of maximum compression of the bellows, at this time, the maximum thrust $F_{\max}$ that the bellows receive is

$$F_{\max} = K_q(X_0 + \Delta L + X). \tag{3}$$

In the formula, K_q represents the stiffness of the bellows.

At this point, the maximum thrust $f_{\max}$ that the micrometer head exerts on the bellows is

$$f_{\max} = K_q(X_0 + \Delta L + X) - F_p. \tag{4}$$

F_p is the thrust on the bellows generated by the pressure difference inside and outside the cryogenic vacuum chamber.

Denoting the maximum distance blade 2 can move to the right as Y, where Y is the position of minimum compression of the bellows, at this time, the minimum thrust $F_{\min}$ that the bellows receives is

$$F_{\min} = K_q(X_0 + \Delta L - Y). \tag{5}$$

At this point, the minimum thrust $f_{\min}$ that the micrometer head exerts on the bellows is

$$f_{\min} = K_q(X_0 + \Delta L - Y) - F_p. \tag{6}$$

The thrust F exerted on the bellows varies during the blade adjustment process, and the range of F is between $F_{\min}$ and $F_{\max}$. The requirement for $F_{\max}$ is that the thrust causes the compression generated by the bellows should be less than its theoretically designed maximum compression. The thrust's reaction force exerted on the micrometer head and its supporting structure should not cause deformation of the micrometer head and its supporting structure. $F_{\min}$ requires that the thrust should ensure that the blade is stable and does not move while the FTIR works.

The maximum amount of compression for the bellows should be less than 0.6 times the natural length L of the bellows, that is, both X and Y should be less than $0.6L$-$(X_0+\Delta L)$, meanwhile, the amount of compression for the bellows should be larger than 0, that is, Y should be less than $X_0+\Delta L$. Select the existing specifications of the bellows from the manufacturer, with a natural length L of 15 mm, and conduct mechanical tests on the bellows. Under one atmospheric pressure, the amount of compression for the bellows is 1.071 mm. The characteristic curve of the bellows is shown in Figure 5. The stiffness K_q of the bellows is 8.31 N mm^{-1}, so $F_p = 8.904$ N.

We can set the adjustment range parameters for the blade, calculate the thrust F that the bellows receive, and check whether the selected parameters are reasonable. Assuming the initial compression amount of the bellows X_0 is 4 mm, the maximum distance X for blade 1 to move left is 2 mm, and the maximum distance Y for blade 2 to move right is 2 mm. From Equations (3) to (6), it can be seen that within the adjustment range, the thrust F that the bellows receive ranges from 50.998 N ($F_{\max}$) to 17.758 N ($F_{\min}$), which can keep the blade from moving while the FTIR works. The micrometer head provides a thrust range from 42.094 N ($f_{\max}$) to 8.854 N ($f_{\min}$). The two micrometer heads are fixed to their support structures by screws, and the support structures are fixed to the substrate. Under the maximum reaction force, the support structures will not deform.

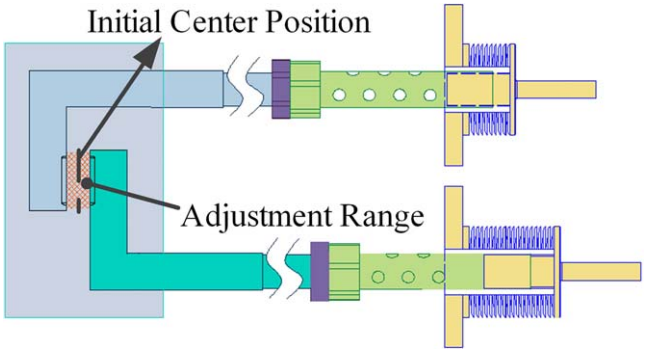

Figure 6. Schematic of adjustment for view field diaphragm.

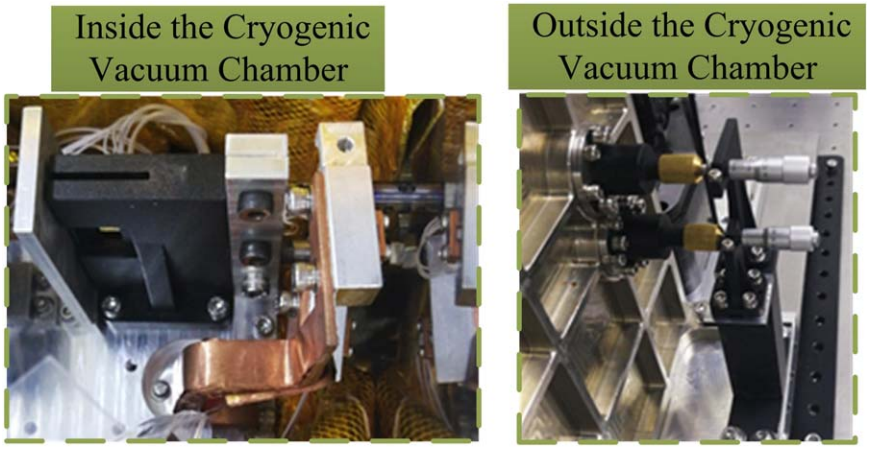

Figure 7. Physical picture of the view field diaphragm installed in the cryogenic vacuum chamber.

In summary, with the initial closed position of the two blades as the center, any position and width of the view field diaphragm can be adjusted within a 2 mm area on both sides, and the structure is stable, as shown in Figure 6. The reading error of the adjustment amount depends on the reading error of the micrometer head. The dividing line of the micrometer head is 0.01 mm, and the visual error of a single dividing line to a double dividing line is not greater than $1/4$ of the dividing line value. Therefore, the displacement reading error of this adjustment mechanism is not greater than 2.5 μm, which is much smaller than the detection element size of 50 μm. For FTIR, the width of the two detectors at this image plane is 0.15 mm, and the adjustment range of the view field diaphragm can cover the application requirements.

4. Experiment

We installed the field diaphragm in the cryogenic vacuum chamber of FTIR, as depicted in Figure 7. The cold optical components inside the cryogenic vacuum chamber are cooled by a pulse tube refrigerator, which is connected to the cold optical substrate through a cold chain, and the diaphragm linkage is connected to the cold optical substrate through a cold chain so that the blade temperature can reach 80 K.

In the FTIR, the arrangement of the detector chips corresponds to the initial position of the view field diaphragm as diagrammed in Figure 8. The view field diaphragm is closed, and a 500°C blackbody is used as the light source. The amplitude of the interference signal collected by the detection element is 0. The detection element corresponds to a tiny field of view in front, though the interference signal is very small. Therefore, the electronic system adopts a gain of 100,000 times, and the electronic bandwidth is not small. So, some electronic noise can be seen when the diaphragm is fully closed, as depicted in Figure 9.

Then fix the bellows 1, rebound bellows 2, and the blade is open, as illustrated in Figure 10. The interference signal of light received on the detector chips is shown in Figure 11. The signal on the even-numbered detector chips in the figure is the interference signal of the beam corresponding to the view field, while the beam on the odd-numbered detector chips corresponding to the view field is blocked by blade 1. The weak interference signal displayed on the odd-numbered detector

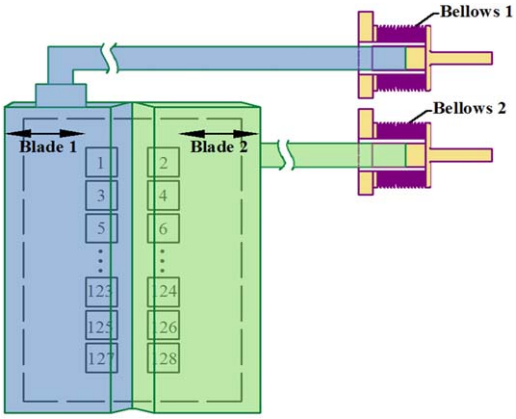

Figure 8. Schematic of the detection element arrangement which corresponds to the initial position of the view field diaphragm.

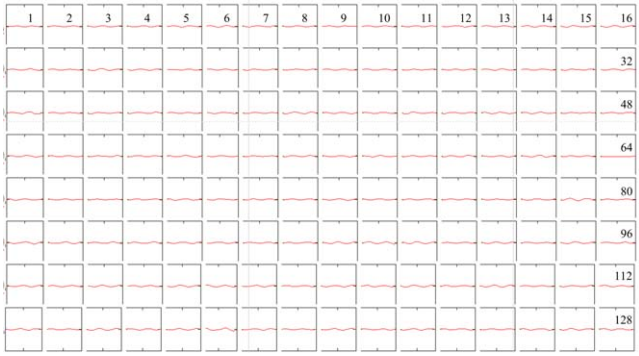

Figure 9. Electronic background signal for each detection element when the view field diaphragm is closed.

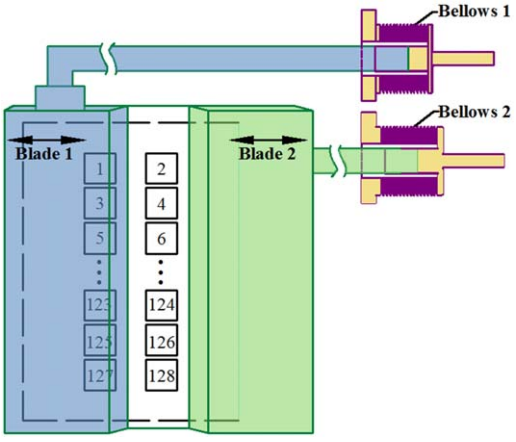

Figure 10. Schematic of opening the blade 2.

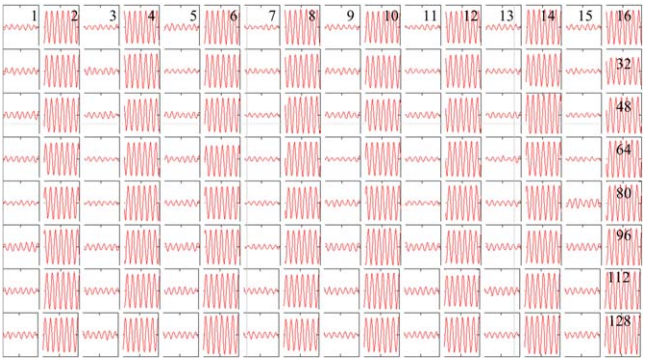

Figure 11. Interference signals when blade 2 of the diaphragm is open.

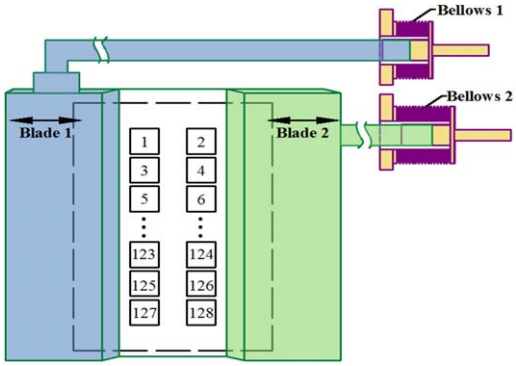

Figure 12. Schematic of opening the blade 1.

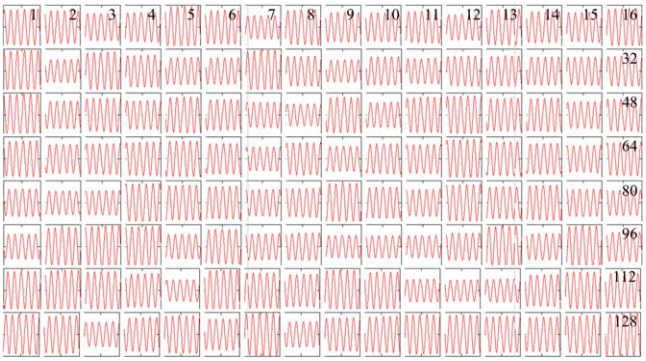

Figure 13. Interference signals when both blade 1 and blade 2 of the diaphragm are open.

chips in Figure 11 comes from the diffraction and scattering effects of the beam passing through the diaphragm.

Lock blade 2, and compress the bellows 1 to open blade 1, as shown in Figure 12. At this time, the interference signals of the beam received on the two columns of detection elements are shown in Figure 13.

The experiment shows that the cold view field diaphragm adjustable method and device explored in this paper can continuously adjust the width and position of the diaphragm.

5. Conclusions

This study has achieved the function of quantitatively adjusting the width and position of the cold view field diaphragm, which can balance the optimal width and position of the view field diaphragm based on the signal size and instrument performance. There are no electronic devices or components in the entire system and no signal interference during the adjustment process. The structure is centralized and low-cost, the adjustment action has no power consumption, and the view field diaphragm can be repeatedly adjusted. The adjustment process will not affect the vacuum degree or the temperature inside the cryogenic vacuum chamber. The adjustment device does not require any lubricating grease, there is no risk of jamming, and it will not cause any pollution to the optical components for long-term use. The diaphragm adjustment can be carried out at low-temperature without re-opening the cryogenic vacuum chamber, which is convenient for improving work efficiency.

For view field diaphragm of slit type, this method can help to find the optimal width and position of the slit through detector chip signal changes, and read the displacement and amount of width adjustment from the micrometer head. In summary, this paper provides a method for studying the optimal slit width and optimizing instrument performance. Meanwhile, this method can block excess light to enter into the system to form stray light. This method has been verified to be correct and feasible by FTIR in AIMS. Similarly, this method can also be applied to other spectrometers that use linear array detectors.

Acknowledgments

This work is supported by the National Natural Science Foundation of China (NSFC, Grant No. 11427901).

References

Ma, N., Liu, Y., Li, J., & Yu, S. 2017, Laser & Infrared, 47, 1195
Nahumn, G., Zhang, J., Li, M., Chen, L., & Hector, G. 2007, Proc. SPIE, 6542, 65420Y
Sun, H., Chen, X., Xia, M., et al. 2024, Infrared Technology, 46, 376, (in Chinese)
Wang, H., Chen, Q., Ma, Z., Yan, H., & Xue, Y. 2022, AcPSi, 51, 0751406
Wang, J., Li, C., Ji, H., et al. 2015, Journ. of Infrared and Millimeter Waves, 34, 51, (in Chinese)
Wei, M., Wang, C., Li, Y., et al. 2020, Infrared and Laser Engineering, 49, 0214004